Complementary Evaluation of Diagonal Tension Field Inclination Angle in Steel Plate Shear Walls

YUSHAN FU and MICHEL BRUNEAU

ABSTRACT

Complementarily to previous studies, research was conducted to investigate whether the equivalent constant angle of diagonal tension field action should be taken as either 40° or 45° for ductile steel plate shear walls (SPSW) designed per current codes. A two-dimensional finite element (FE) model was first calibrated against results from a prior study of "limited-ductility SPSW" by comparing effective stress contours and average angle of diagonal tension field action at different locations across the web plate. Then, this SPSW was redesigned as a ductile SPSW in compliance with the 2016 AISC *Seismic Provisions* (AISC, 2016a) to have fully restrained beam-to-column connections and analyzed using strip models and finite element models, respectively. The AISC moment-axial force interaction equation was used to compare demands in the SPSW boundary elements obtained from the strip and finite element models. With respect to the use of a single angle in design, it is shown that using an inclination angle of 45° is slightly (but not significantly) more conservative than using 40° as far as boundary element design is concerned. On the basis of these observations, along with findings from previous research on the diagonal tension field inclination angle, it is recommended that a single constant angle of either 40°or 45° be used for the design of SPSW.

Keywords: steel, plate, shear, wall, inclination angle, tension, field, LS-DYNA, seismic design, ductile design.

INTRODUCTION

Steel plate shear walls (SPSW) are one of the newest lateral load-resisting structural systems introduced in the AISC *Seismic Provisions* (AISC, 2005, 2010, 2016a), on the strength of extensive research in the past decades (e.g., Astaneh, 2004; Behbahanifard et al., 2003; Berman and Bruneau, 2004; Choi and Park, 2009; Driver et al., 1997a, 1997b; Elgaaly et al., 1993; Rezai, 1999; Roberts and Sabouri-Ghomi, 1992; Timler and Kulak, 1983; to name a few). These provisions address SPSW with unstiffened infill plates (i.e., plates functioning as webs) having large width-to-thickness ratios and relying on the development of inelastic diagonal tension field action to resist lateral loads and provide hysteretic energy dissipation during earthquakes. The orientation of the post-buckling principal stresses that develop in the infill plates of SPSW due to this tension-field action varies in a complex manner as a function of drift, location along boundary elements, and stages of inelastic behavior (Fu et al., 2017; Webster, 2013; Webster et al., 2014).

Yushan Fu, Graduate Research Assistant, Department of CSEE, University at Buffalo, Amherst, NY. Email: yushanfu@buffalo.edu (corresponding)

Michel Bruneau, Professor, Department of CSEE, University at Buffalo, Amherst, NY. Email: bruneau@buffalo.edu

Paper No. 2018-02

Pushover analysis of nonlinear, inelastic, finite element models can capture these variations as a function of drift and other SPSW properties, but this is not a practical tool for design. To simplify this complex behavior of SPSW in a manner suitable for design, Thorburn et al. (1983) proposed a strip model that replaces the infill plates with diagonal strips. In that model, at a given story, all the strips are oriented at the same angle from the vertical. In various editions of the AISC *Seismic Provisions* (and CSA S16) (see CSA, 2001, 2009, 2014), an equation has been provided to determine the angle to be used in the strip model; this equation was derived by Thorburn et al. (1983) [and later refined by Timler and Kulak (1983)] considering the relative elastic flexibility of boundary elements surrounding a panel. Using this equation typically leads to different angles used at the different stories along the height of an SPSW. To further simplify design, the AISC *Seismic Provisions* have allowed that a single angle could be used over the entire height (AISC, 2005). Initially, the provisions indicated that this value could be taken as equal to the average of all values calculated over the SPSW height; subsequently, using a constant angle of 40° was permitted, based on a study by Shishkin et al. (2005) described later.

Since then, other researchers have investigated whether using an equivalent constant angle of diagonal tension field action of 45° may be also appropriate for design as an alternative to the value of 40° currently permitted for ductile SPSW designed according to the current AISC *Seismic Provisions* and CSA S16 (2014). From a practicing engineer's perspective, using an angle of 45° is advantageous because it facilitates construction of the strip models for the SPSW. Past results, focusing on simplified one-story SPSW having

a 1:1 aspect ratio (Webster, 2013; Webster et al., 2014), suggested that it would be appropriate; a subsequent study considering a number of code-compliant SPSW of different configurations, and comparing demands from the web plate on individual elements [Fu et al. (2017)] recommended using a constant angle of 45°. To answer the remaining question on this topic, the results presented here expand on this past research by investigating demands on the boundary elements of ductile SPSW designed according to the latest AISC *Seismic Provisions* requirements, by comparing results in terms of the complete system-induced demands in each members and using axial-bending interaction equation from AISC *Specification* Section H1.1 (AISC, 2016b).

More specifically, this paper first reviews the literature related to definition of the angle to use in SPSW strip models and then uses results from one of these studies to calibrate a finite element model to replicate past results and to investigate demands on the boundary elements of some ductile SPSW. Results obtained from finite element analysis and from strip models using either 40° or 45° are then compared to assess the significance of the differences.

LITERATURE REVIEW

The current AISC *Seismic Provisions* (2016a) and CSA S16 (2014) specify that the inclination angle of the diagonal tension field measured from the vertical can be calculated by the Equation 1 derived from elastic strain energy principles in Timler and Kulak (1983) as:

$$\tan^4 \alpha = \frac{1+\frac{t_w L}{2A_c}}{1+t_w h\left(\frac{1}{A_b}+\frac{h^3}{360 I_c L}\right)} \quad (1)$$

where

A_b = cross-sectional area of the horizontal boundary element (HBE), in.^{2} (mm^2)

A_c = cross-sectional area of the vertical boundary element (VBE), in.^{2} (mm^2)

I_c = moment of inertia of the VBE, in.^{4} (mm^4)

L = bay width, in. (mm)

h = story height, in. (mm)

t_w = thickness of the infill plate, in. (mm)

However, the fact that this equation was derived considering the elastic flexibility of a simplified subassembly is sometimes forgotten, and its complexity may inadvertently provide a disproportionate sense of accuracy, which is counter to the variations in actual angle observed in nonlinear analyses (specifically, those in the research summarized later).

Subsequently, Shishkin et al. (2005) suggested that a constant 40° angle could be used throughout by investigating the nonlinear behavioral effects of using various constant inclination angles on 1-story, 4-story, and 15-story SPSW strip models. These SPSW were designed to have an aspect ratio between 0.75 and 2.0, column flexibility factors (defined by the 2016 AISC *Seismic Provisions* Section F5.4a) ranging between 1.3 and 3.1, and either fully restrained (stated as being "rigidly connected" in the AISC *Seismic Provision* Commentary) or pinned beam-to-column connections (except for the 15-story SPSW, which were only considered with fully restrained moment-resisting connections), as part of a parametric study. Constant angles of 38° and 50°, permitted by CSA S16-01 (2001) were considered over the structure's height. Results showed that the angle of the tension strips had little impact on the predicted ultimate strength of an SPSW. Because the 38° models behaved somewhat more flexibly than the 50° models, the 40° value was recommended as a constant value for future designs. However, only the preceding two values of angles were considered for the strip models during the parametric studies, and comparisons focused on the ultimate strengths and initial stiffness of SPSW (without comparison against finite element results).

Later studies by Moghimi and Driver (2014a, 2014b) investigated a proposed alternative type of SPSW having moderately ductile behavior to be used in low seismic regions as a possible alternative to the existing SPSW in CSA S16-09 (having performance levels defined as "Type D" for "ductile plate walls" and "Type LD" for "limited ductility plate walls") and the 2010 AISC *Seismic Provisions* ("special plate shear walls"). One part of this study addressed the inclination angle of the diagonal tension field of a hypothetical four-story type LD SPSW designed per CSA S16 (2009). Results showed that the mean value of the angle α at the ultimate capacity of the wall (defined as occurring at 2.5% drift in that study) tended to be close to 39° and 51° adjacent to the beam [horizontal boundary element (HBE)] and compression column [vertical boundary element (VBE)], respectively. In addition, the effect of the minor principal compression stresses (σ_2) on demands for the boundary elements was investigated. It was observed that due to the von Mises yield criterion, the presence of σ_2 compression stresses led to an earlier tension yielding of the web plate around the boundary elements. It was reported that this simultaneously resulted in an increase of the forces applied (by the yielding infill) perpendicular to the boundary elements and a decrease of the forces applied parallel to the boundary elements. It was indicated that using 40° for the inclination angle, together with considering σ_2 and its effects on F_y and on the strip model, would provide acceptable and conservative results for the HBE, VBE, and web design. However, modifying the strip model this way, through determination

of σ_2 and considering the von Mises interaction, might be demanding from a practical perspective.

Webster et al. (2014) conducted both experimental and analytical analyses on two one-story SPSW having pinned HBE-to-VBE connections, slender VBEs, and cutouts at the web plate corners. The variation of the inclination angle of the diagonal tension field action acting in the SPSW was presented as a function of drift. By averaging the inclination angles over single panels, the mean was found to approach a value between 43° and 45°. For simplicity, use of a constant 45° angle was recommended by Webster et al. for capacity design procedure and cyclic analysis of SPSW systems. However, it was unknown how these findings would be affected when using moment-resisting HBE-to-VBE connections and how results would change for walls having different aspect ratios and number of stories.

To expand on the Webster et al. (2014) studies and to better understand how the inclination angles varied at different locations over the web plate and how this influenced demands of HBEs and VBEs for different SPSW configurations designed according to the AISC *Seismic Provisions*, Fu et al. (2017) investigated variations of the inclination angle in four AISC-compliant SPSW having aspect ratios of 1 and 2 and either one or three stories, using nonlinear, inelastic, finite element analysis. Similarly to what was reported by Moghimi and Driver (2014b), it was observed that the average inclination angles varied between 35° and 45° along the HBE and between 45° and 65° along the VBE. Beyond that, the inclination angles were also observed to vary as a function of drifts, panel aspect ratios, and numbers of stories.

For example, comparing results using a proposed combined moment-axial force ratio, it was shown that changing the aspect ratio had a significant impact on the level of conservatism obtained in respective three-story SPSW when comparing results for analyses using the same constant angles. As the number of stories increased, the ratios calculated for the top HBEs changed from being conservative to being unconservative, whereas observations for the tension VBEs were just the opposite. Using strips oriented at 35° and 40° for HBE design and 50° for VBE design were always found to be conservative. In the perspective that a single angle is used in modeling a SPSW, it was also observed that using a single angle of 45° provided a good compromise for both HBE and VBE design. Furthermore, because the demand on web plate is not sensitive to the variation of inclination angle, a single value of 45° was recommended for the design of the entire SPSW. However, in that study, calculation of combined moment-axial force ratio was done on an element basis, accounting for the stresses induced from the web plate but without consideration of force and moment interactions between HBEs and VBEs. This shortcoming is resolved by the research presented next.

MODEL CALIBRATION

Previous research in Fu et al. (2017) investigated the development of the diagonal tension field action and its orientation based on the calibration of the one-story SPSW experimentally and numerically studied in Webster et al. (2014), in order to match the variation of the average inclination angle over a single panel as a function of drift. That model was then modified to model AISC-compliant SPSW and used to perform the research described earlier. For the complementary work presented here and to broaden the validity of the findings in Fu et al., the numerical analyses began with calibration of an LS-DYNA model to replicate those from the limited-ductility, four-story SPSW designed with pinned beam-to-column connections and analyzed using ABAQUS by Moghimi and Driver (2014b), for which the distribution of inclination angle over the entire web plate was provided. This was done because that study is the only one advocating the use of the 40° angle for which finite element analyses were conducted. Then, after comparison of the results showed the LS-DYNA to match those reported by Moghimi and Driver (2014b), the LS-DYNA model was modified to have fully restrained HBE-to-VBE connections in compliance with the current AISC seismic design specifications. Note that line elements were used here for the HBEs and VBEs in the LS-DYNA model to be consistent with the approach used by Moghimi and Driver (2014b). Then, two strip models were constructed using SAP2000: one with strip inclination angle of 40° and one with 45°. To account for the actual demands of the HBEs and VBEs, forces and moments were output directly from LS-DYNA and SAP2000 for comparison, and the AISC moment-axial force interaction equation was used to evaluate the conservatism of the resulting demands for the HBE and VBE design. Details of these analyses are presented next.

Dimensions and Boundary Conditions

The finite element model, developed using LS-DYNA, for the limited-ductility, four-story SPSW studied by Moghimi and Driver (2014b) is presented in Figure 1. The bay width of the SPSW is 236.22 in. (6000 mm), and the story heights are 165.35 in. (4200 mm) and 145.67 in. (3700 mm) for the first story and the other three stories, respectively. The sections designed according to the AISC *Seismic Provisions* (2010) for the fourth-story and second-story HBEs are W24×306 and W12×190, respectively, while W10×100 are used for both the first-story and third-story HBEs. A built-up VBE having 19.69-in. × 0.79-in. (500 mm × 20 mm) flanges and 19.69-in. × 1.97-in. (500 mm × 50 mm) web was used. The base of the wall was modeled to be continuously fixed. The thicknesses of the web plates were 0.19 in. (4.8 mm) for the third and fourth stories and 0.25 in. (6.4 mm) for the first and second stories.

Material and Element

Similarly to what was done with the ABAQUS modeling in Moghimi and Driver (2014b), the four-node Belytschko-Tsay shell element was chosen for the web plate, and the Hughes-Liu beam element with 15 cross-section integration points was selected for the HBEs and VBEs. The HBEs were pin-connected to the adjacent VBEs by releasing the in-plane rotation at the HBE ends, as shown in Figure 1. The web plates were extended to the edge of the surrounding boundary elements to account for offsets in the connection points, and each node at the edge of web plates was constrained to the corresponding node on the centerline of the boundary element in its six degrees of freedom (DOF) through NODAL_RIGID_BODY_SPC. The out-of-plane translational and rotational DOF of the nodes along HBEs and VBEs were fixed. An elastic-plastic constitutive model without strain hardening was specified for the steel web plate using MAT024_PIECEWISE_LINEAR_PLASTICITY. Boundary elements were modeled with an elastic-plastic model having 1% isotropic strain hardening, defined using MAT003-PLASTIC-KINEMATIC_ISOTROPIC HARDENING. The specified material had a Young's modulus of 29,008 ksi (200,000 MPa), a yielding strength of 55.84 ksi (385 MPa), a Poisson ratio of 0.30, and a density of 490.06 lb/ft^3 (7850 kg/m^3).

Loading Protocol

In order to achieve the same roof drift at which the average inclination angle was reported in Moghimi and Driver (2014b), a horizontal force of 472 kip (2100 kN) was first applied at the right HBE end of each story using force control until the converge failure occurred (typically when 0.2% roof drift was reached). The nodal displacements at the right HBE ends on the last step of that analysis were output and then applied proportionally using displacement control up to 2.5% roof drift. These results obtained from the LS-DYNA model using displacement control at 2.5% roof drift are compared with the Moghimi and Driver results next.

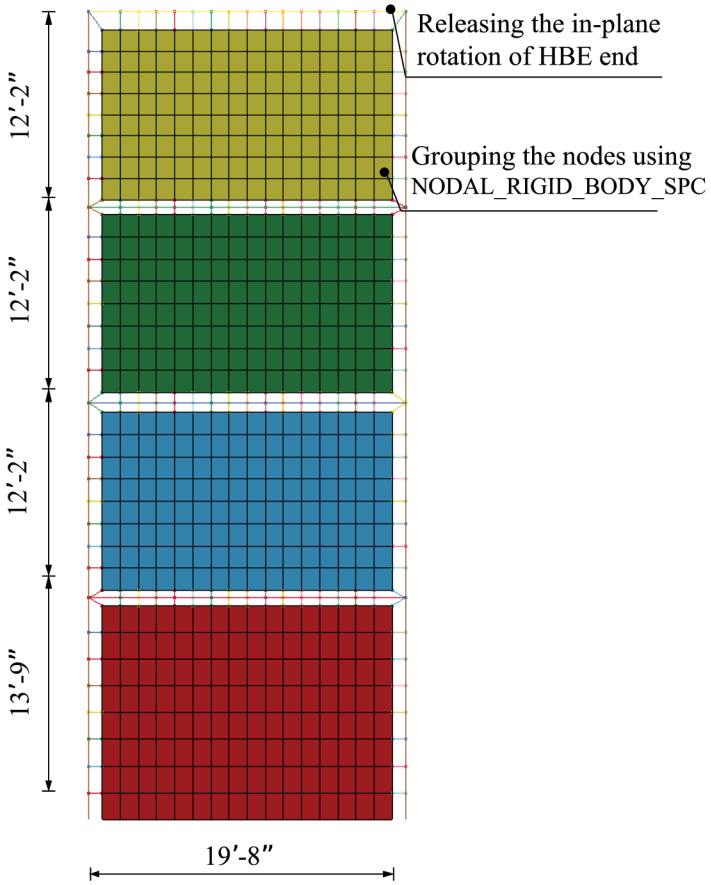

Fig. 1. Dimensions and constraints of four-story, limited-ductility SPSW.

RESULTS FROM CALIBRATION

Von Mises Stress and Effective Plastic Strain Contour

The von Mises contour and principal stress vector presented in Figure 2 show that all the web plates yielded at 1.9% roof drift. Subsequently, plotted in Figure 3 are the effective strain contours at the roof drifts of 1.9% and 2.5%, respectively. For comparison, Figure 3(c) shows the effective plastic strain contour at 2.5% drift from Moghimi and Driver (2014b); the contours and magnitude of the effective plastic strains obtained from both models are in good agreement in capturing the behavior of the limited-ductility SPSW. It also illustrates that the distribution of effective strains in that system is more severe and concentrated near the right VBE, which is different from the more uniform strain distribution that develops across the entire web of ductile SPSW designed according to the 2016 AISC *Seismic Provisions*.

Inclination Angle Analysis

From the preceding finite element analysis, the inclination angle was calculated from the resulting in-plane stresses for each shell element considered. Focusing on the areas of interest here, the inclination angle of the diagonal tension field was averaged along the HBEs and VBEs, as well as along the mid-web region used in Moghimi and Driver (2014b). Figure 4 shows that all the curves vary extensively as a function of drift [consistently to what was reported by Fu et al. (2017)] and tend to converge at 2.5% roof drift, as the average inclination angle approached 40° for the HBE, 52° for the VBE, and 47° at the middle of the web.

INCLINATION ANGLE FOR DUCTILE SPSW

Ductile SPSW in Compliance with the AISC *Seismic Provisions*

To investigate the effects of the inclination angle used in the strip models for the design of ductile SPSW, the preceding SPSW was redesigned to have fully restrained HBE-to-VBE connections in compliance with the AISC *Seismic Provisions* (AISC, 2016a) and using the constant angle of 40°. HBEs and VBEs were designed to resist combined flexure and axial compression. The HBE was sized to resist forces determined from the capacity design procedure, while the VBEs were selected based on results of the pushover analyses conducted in SAP2000. Figure 5 illustrates the two kinds of pushover analyses conducted for this purpose. The selection of the load patterns adopted in this research was inspired by Krawinkler and Seneviratna (1998), who showed that no unique load pattern in pushover analysis is capable of bounding the distribution of inertia forces in a design earthquake, especially in the perspective of inelastic deformations. Using

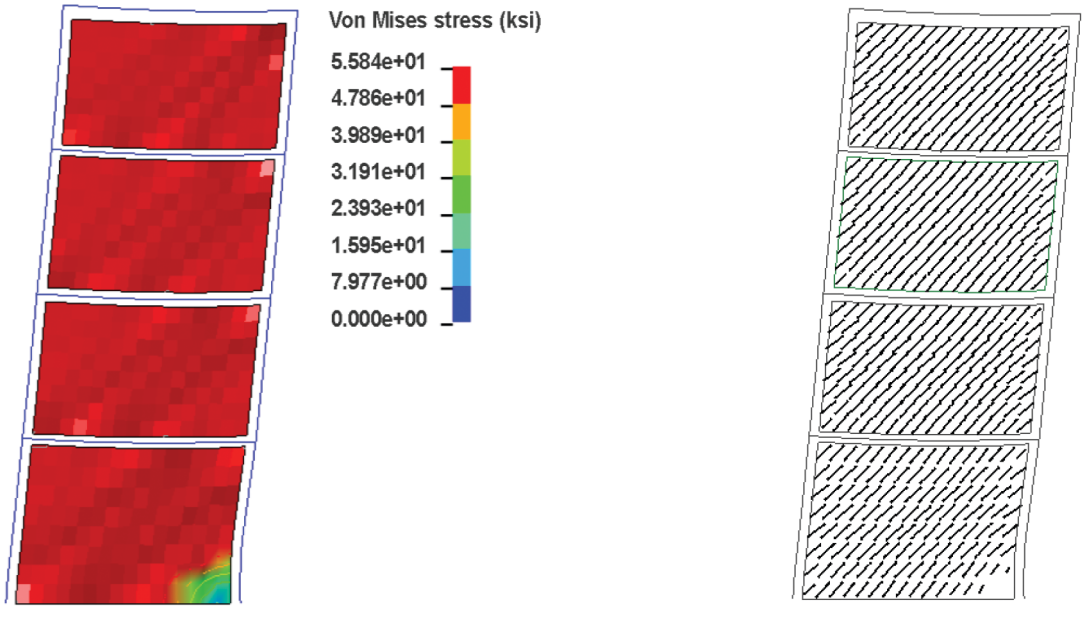

Fig. 2. Von Mises stress contour and principal stress vector: (a) von Mises contour at yield mechanism (1.9% drift) from LS-DYNA model (displacement scale factor = 5); (b) principal stress vector at yield mechanism from LS-DYNA model (displacement scale factor = 5 and vector scale factor = 0.2).

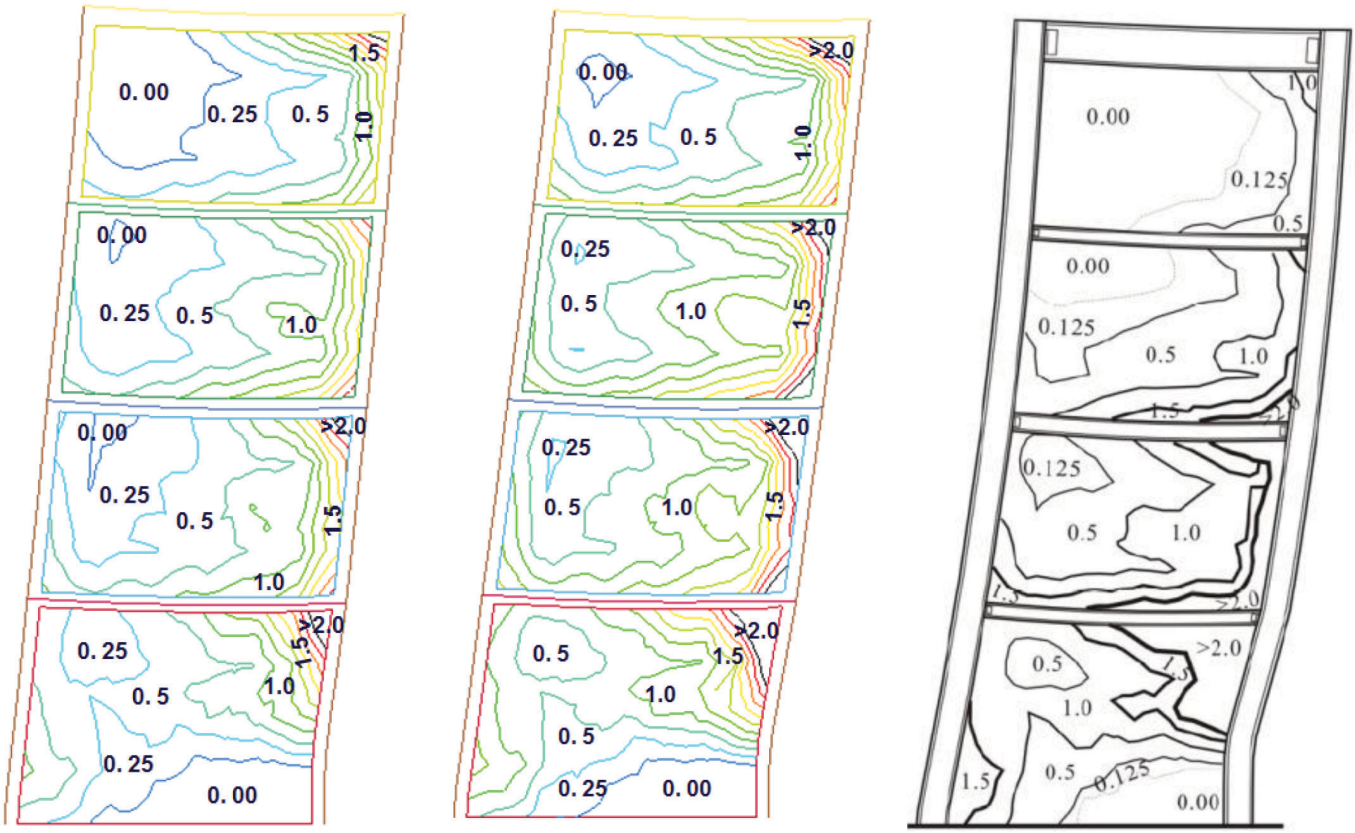

Fig. 3. Comparison on effective plastic strain contours: (a) effective plastic strain contour at yield mechanism (1.9% drift) from LS-DYNA model (%, displacement scale factor = 5); (b) effective plastic strain contour at 2.5% drift from LS-DYNA model (%, displacement scale factor = 5); (c) effective plastic strain contour at 2.5% drift from Moghimi and Driver (2014b) (%).

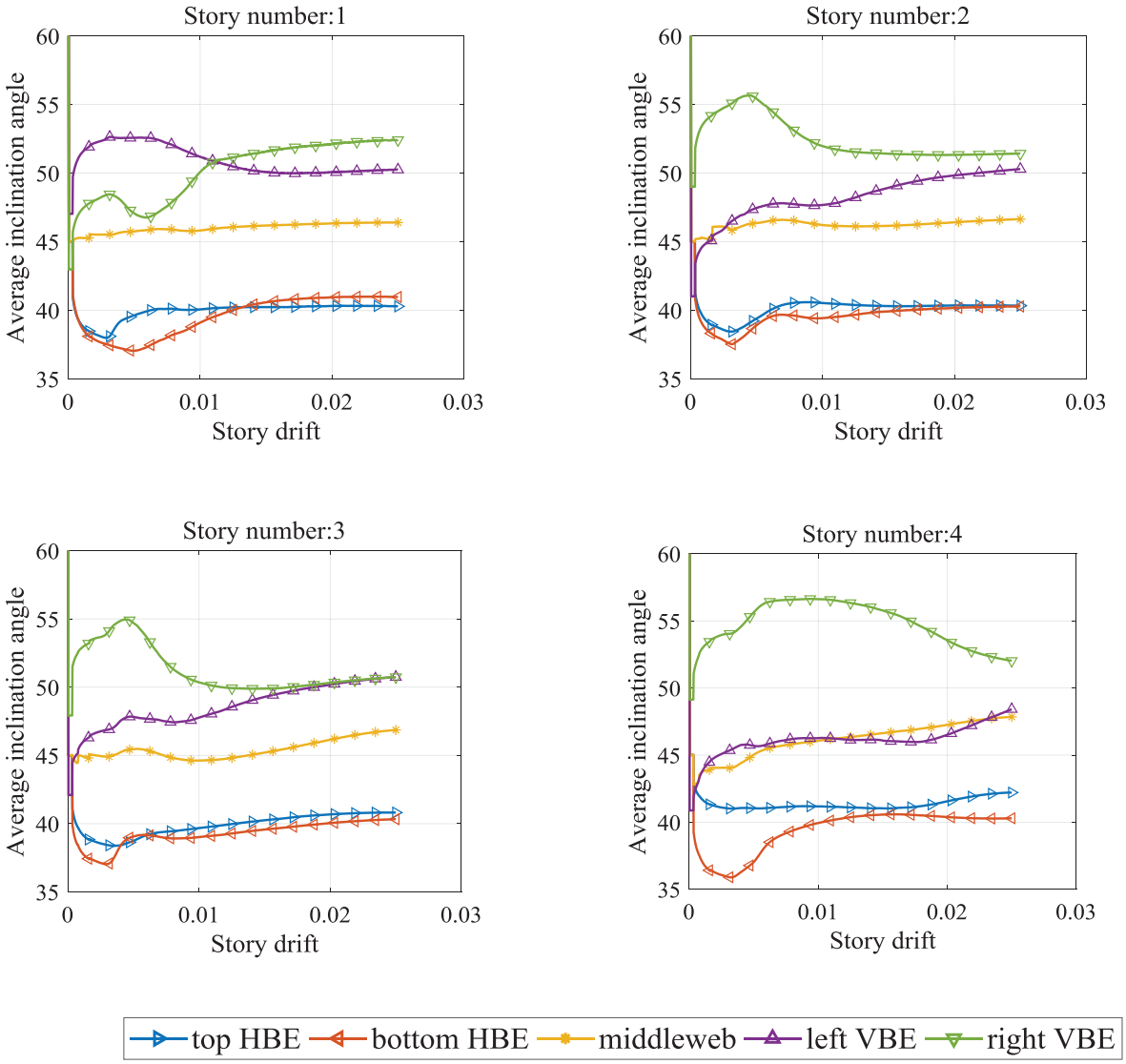

Fig. 4. Inclination angle variation.

different load patterns allows for investigating the variation of the inclination angle under those conditions as drift increases and for examining the conservativeness of using a constant angle over the structure height in such cases. Therefore, two recommended load patterns—namely, a uniform distribution of load and an inverted triangular load—were applied here. In the former case, a horizontal force of 400 kips (1779 kN) was applied at each end of the HBEs; plastic hinges were observed to have developed at the ends of all HBEs and at the base of the VBEs when displacement at the mid-point of the fourth-story HBE reached 2.5% roof drift. In the latter case, the load pattern was achieved by applying an increasing unidirectional ground acceleration until the mid-point of the fourth-story HBE reached 2.5% roof drift and the same yield mechanism was observed to have occurred. Hereafter, the SAP2000 models designed with constant angle of α and subjected to either uniform distribution or inverted triangular forces are referred to as SP-α-U and SP-α-T, respectively. Note that for the HBEs to which the web plates above and below have the same thickness (namely, the first and third HBEs in this example), design was governed by axial demands as well as by the requirement that the moment-resisting frame alone be able to carry at least 25% of the seismic base shear, which was verified by using a SAP2000 model of the bare frame consisting of the HBEs and VBEs alone.

SAP2000 Modeling of Ductile SPSW

The constitutive models used for the boundary elements and strips in the SAP2000 models were the same as those in the calibrated LS-DYNA model (described earlier). Fourteen strips were selected for each story for all the strip models. The nonlinear behavior of the tension-only-strip was achieved by applying a compression limit on the strip and releasing the rotational DOF at the strip ends. Plastic hinges were defined using P-M2-M3 hinges at both ends of each HBE and VBE to capture their nonlinear behavior.

For the redesigned SPSW, the resulting fourth-story to first-story HBEs (top to bottom) were W40×397, W12×170, W33×241, and W12×170, respectively. A single built-up VBE cross section was used along the height, with a depth d = 44.52 in. (1130.70 mm), flange width b_f = 19.33 in. (491.05 mm), flange thickness t_f = 3.89 in. (98.91 mm), and web thickness t_w = 2.17 in. (55.04 mm).

LS-DYNA Modeling of Ductile SPSW

The ductile SPSW was similarly modeled using the calibrated LS-DYNA model mentioned earlier but with some differences in the constraint, mesh and loading protocols. First, fully restrained HBE-to-VBE connections were achieved by fixing the in-plane rotation at the HBE ends. In order to capture the behavior of plastic hinges, the size of the mesh at the HBE and VBE ends was determined based on the results from a separate study on a cantilever column, comparing the difference between base moments obtained from LS-DYNA and SAP2000. In addition, 27 integration points (nine points for each flange and nine points for the web) were applied on the beam element cross-section, as a refinement from the 15 used previously.

Comparison of Results from Finite Element Analysis and Strip Models

The SPSW designed in compliance with the 2016 AISC *Seismic Provisions* (as described earlier) was analyzed using both the LS-DYNA model described in the previous section and SAP2000 models having strips oriented at the same angle throughout (one analysis with strips at 40° and one analysis with strips at 45°). To be able to compare the results obtained using the strip models with the ones obtained using the finite element, the displacement histories obtained from SP-40°-U, SP-40°-T, SP-45°-U and SP-45°-T, in addition to the lateral loads, were applied to the corresponding LS-DYNA models, as described in Figure 5.

The appropriateness of demands from modeling using 40° and 45° in the strip model was evaluated by comparing the demands on the HBEs and VBEs obtained from SAP2000 with the corresponding demands from LS-DYNA. For this purpose, the demands obtained by considering the 2016 AISC *Specification* combined moment-axial force interaction equation were compared. For large axial load ($P_{FE}/P_{CD} \geq 0.2$), this was effectively achieved by calculating the following ratio:

$$\frac{\frac{8}{9}\left(\frac{M_{FE}}{M_{CD}}\right)+\frac{P_{FE}}{P_{CD}}}{\frac{8}{9}\left(\frac{M_{strip_\alpha}}{M_{CD}}\right)+\frac{P_{strip_\alpha}}{P_{CD}}} \tag{2}$$

where P_{FE} and M_{FE} are forces and moments obtained from LS-DYNA, P_{CD} and M_{CD} are axial and flexural strength of the frame members, and P_{strip_α} and M_{strip_α} are forces and moments obtained from SAP2000 designed using α = 40° in one case and α = 45° in the other. The inclination angle used for the design is deemed to give conservative results compared to finite element results when the preceding combined moment-axial force demand ratio is less than or equal to 1. Furthermore, for the design to be deemed satisfactory, the ratios from the individual interaction equations in the numerator and denominator must also respectively give results less than or equal to 1.

Tables 1 and 2 present the combined moment-axial force demand ratios calculated for the HBEs, left VBE, and right VBE at each story, denoting the left and right end of the HBE as HBEL and HBER and the top and bottom of the VBE as VBET and VBEB. The ratios of (FE/CD) and (Strip/

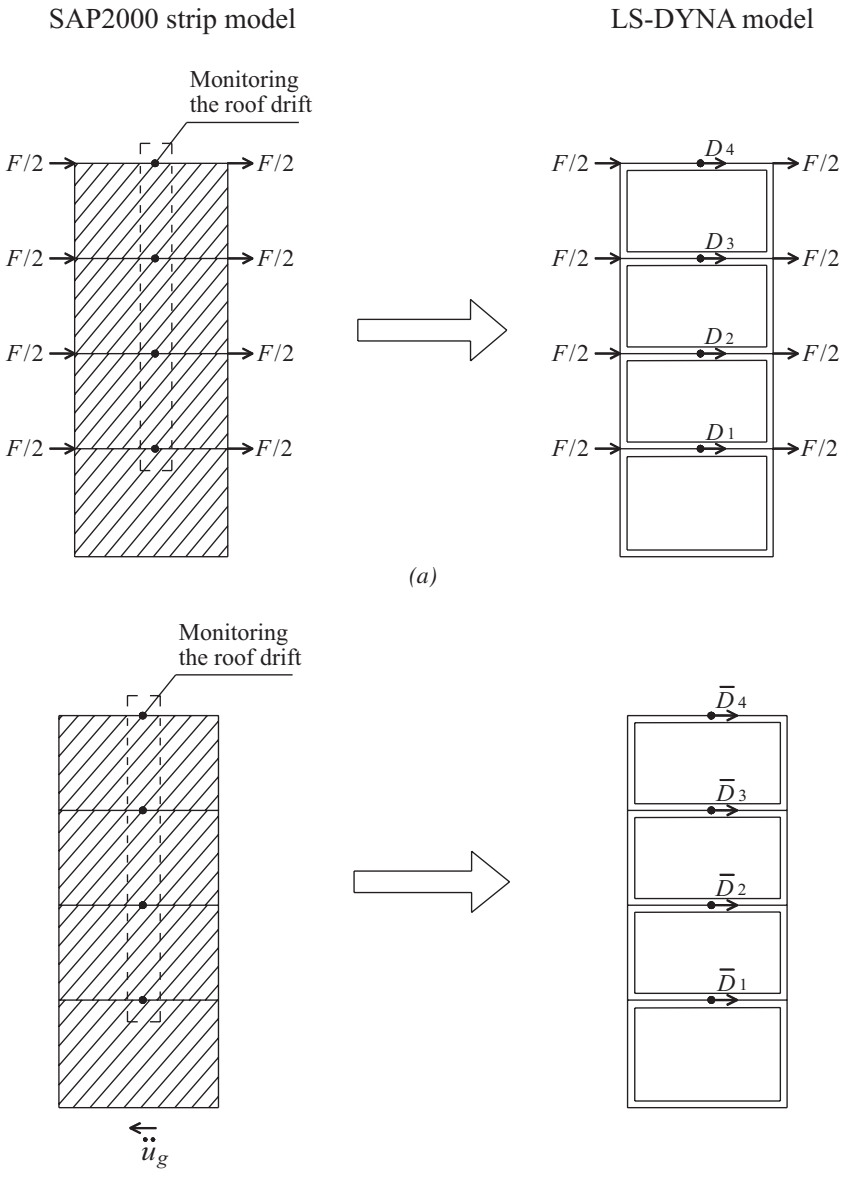

Fig. 5. Loading approaches for pushover analyses in SAP2000 and LS-DYNA: (a) uniform distribution of force; (b) inverted triangular force. D and $\overline{D}$ refer to displacement histories from SAP2000 model subjected to uniform distribution of force (SP-40°-U and SP-45°-U) and inverted triangular force (SP-40°-T and SP-45°-T), respectively.

Table 1. Combined Moment-Axial Demand Ratio of the SPSW Subjected to Pushover Analysis Using Uniform Lateral Load (Comparing SP-40°-U and SP-45°-U with the LS-DYNA Model Subjected to the Pushover Displacements and Loads from SP-40°-U)									
HBE	**Location**	**4th HBEL**	**4th HBER**	**3rd HBEL**	**3rd HBER**	**2nd HBEL**	**2nd HBER**	**1st HBEL**	**1st HBER**
	*Rb*_40°	1.08	0.91	0.91	0.94	0.92	0.91	0.83	0.94
	FE/CD	0.83	0.84	0.87	0.89	0.97	0.90	0.86	0.97
	Strip/CD	0.77	0.92	0.96	0.95	1.06	0.99	1.05	1.04
	*Rb*_45°	1.12	0.91	0.87	0.90	0.91	0.89	0.82	0.92
	FE/CD	0.83	0.84	0.87	0.89	0.97	0.90	0.86	0.97
	Strip/CD	0.74	0.92	1.00	0.98	1.07	1.02	1.06	1.06
VBE (L)	**Location**	**4th VBET**	**4th VBEB**	**3rd VBET**	**3rd VBEB**	**2nd VBET**	**2nd VBEB**	**1st VBET**	**1st VBEB**
	*RcL*_40°	1.22	0.99	1.02	0.88	0.94	1.19	1.25	1.00
	FE/CD	0.38	0.44	0.51	0.32	0.55	0.30	0.38	1.10
	Strip/CD	0.31	0.44	0.50	0.37	0.58	0.25	0.30	1.10
	*RcL*_45°	1.28	1.02	1.07	0.86	0.92	1.07	1.18	0.99
	FE/CD	0.38	0.44	0.51	0.32	0.55	0.30	0.38	1.10
	Strip/CD	0.30	0.43	0.47	0.37	0.59	0.28	0.32	1.11
VBE (R)	**Location**	**4th VBET**	**4th VBEB**	**3rd VBET**	**3rd VBEB**	**2nd VBET**	**2nd VBEB**	**1st VBET**	**1st VBEB**
	*RcR*_40°	0.91	0.88	0.91	1.00	0.98	1.12	1.10	1.02
	FE/CD	0.48	0.55	0.62	0.46	0.72	0.43	0.50	1.12
	Strip/CD	0.53	0.63	0.69	0.46	0.73	0.39	0.46	1.10
	*RcR*_45°	0.93	0.84	0.87	0.94	0.94	1.04	1.03	1.02
	FE/CD	0.48	0.55	0.62	0.46	0.72	0.43	0.50	1.12
	Strip/CD	0.52	0.66	0.72	0.49	0.76	0.42	0.48	1.10

CD) refer to the values calculated from the nominator and denominator of Equation 2, respectively, while the Rx_α illustrates the resulting ratio from Equation 2 in certain locations (where X is replaced by b, cL and cR to represent the beam, left column, and right column, respectively) using the constant angle α for the strip model. Note that only the results obtained from LS-DYNA models subjected to SP-40°-U and SP-40°-T pushover displacements and loads are presented in Tables 1 and 2 because similar results were obtained when using the LS-DYNA models subjected to those from the 45° cases. As can be seen from the ratios for HBEs, in most of the cases (except for the left end of the fourth-story HBE), using the inclination angle of 45° for design is slightly (but not significantly) more conservative than using 40°; more specifically, compared to results from finite element analysis, demands from forces obtained from the strip model are, on average, 1.3% larger when using 45° as inclination of the strips instead of 40°. Similar observations are obtained for the right VBEs, with results being, on average, 3.7% larger when using 45° instead of 40°. With respect to the left VBEs, although using the angle of 45° is shown to be more conservative only for the third and lower stories, the web in the fourth story was found to be incompletely yielded because the same cross-section was used for all columns.

Table 2. Combined Moment-Axial Demand Ratio of the SPSW Subjected to Pushover Analysis Using Inverted-Triangular Lateral Load (Comparing SP-40°-T and SP-45°-T with the LS-DYNA Model Subjected to the Pushover Displacements from SP-40°-T)									
HBE	**Location**	**4th HBEL**	**4th HBER**	**3rd HBEL**	**3rd HBER**	**2nd HBEL**	**2nd HBER**	**1st HBEL**	**1st HBER**
	*Rb*_40°	1.14	0.97	0.84	1.02	0.83	1.00	0.70	0.95
	FE/CD	0.71	0.84	0.73	0.95	0.87	1.00	0.73	0.99
	Strip/CD	0.62	0.87	0.86	0.93	1.04	1.01	1.04	1.04
	*Rb*_45°	1.21	1.00	0.79	0.97	0.82	0.97	0.69	0.93
	FE/CD	0.71	0.84	0.73	0.95	0.87	1.00	0.73	0.99
	Strip/CD	0.58	0.85	0.92	0.98	1.06	1.04	1.05	1.06
VBE (L)	**Location**	**4th VBET**	**4th VBEB**	**3rd VBET**	**3rd VBEB**	**2nd VBET**	**2nd VBEB**	**1st VBET**	**1st VBEB**
	*RcL*_40°	1.34	1.00	1.05	0.94	0.98	1.13	1.18	1.00
	FE/CD	0.34	0.46	0.53	0.39	0.62	0.34	0.42	1.10
	Strip/CD	0.25	0.46	0.51	0.41	0.63	0.30	0.35	1.10
	*RcL*_45°	1.44	1.06	1.12	0.94	0.98	1.05	1.14	0.99
	FE/CD	0.34	0.46	0.53	0.39	0.62	0.34	0.42	1.10
	Strip/CD	0.24	0.43	0.47	0.42	0.64	0.33	0.37	1.11
VBE (R)	**Location**	**4th VBET**	**4th VBEB**	**3rd VBET**	**3rd VBEB**	**2nd VBET**	**2nd VBEB**	**1st VBET**	**1st VBEB**
	*RcR*_40°	0.93	0.89	0.92	1.05	1.00	1.11	1.07	1.02
	FE/CD	0.48	0.58	0.64	0.53	0.78	0.48	0.53	1.13
	Strip/CD	0.51	0.65	0.70	0.51	0.79	0.43	0.50	1.10
	*RcR*_45°	0.97	0.85	0.88	0.98	0.97	1.04	1.01	1.02
	FE/CD	0.48	0.58	0.64	0.53	0.78	0.48	0.53	1.13
	Strip/CD	0.49	0.68	0.73	0.54	0.81	0.46	0.53	1.10

Comparison of the Forces and Moments Obtained from SAP2000 and LS-DYNA

As noticed in Tables 1 and 2, in most cases, the FE/CD ratios are smaller than the Strip/CD ones, except for some of the ratios in the first and fourth stories. To investigate possible causes for these differences in the FE/CD and Strip/CD ratios, results obtained from the SP-40°-U and SP-45°-U analyses were further compared with those from the LS-DYNA model subjected to pushover displacements and loads corresponding to SP-40°-U. For this purpose, forces and moments acting on the boundary elements at the fourth story are compared in Figure 6, more specifically focusing on the possible role of (as described later) (1) the incomplete yielding of infill at the fourth floor, as revealed by the nonyielded strips near the corners of the infill in the applied parallel and normal force diagrams in Figure 6; (2) the small discrepancy in the displacements obtained in the LS-DYNA model compared to the SAP2000 model as indicated in the axial force plot of Figure 6(a); and (3) the σ_2 effects included in the LS-DYNA model and variation of the inclination angle along the boundary elements.

The applied parallel forces obtained from the SAP2000 strip model indicate that some strips near the top-right and bottom-left corners in the fourth story did not completely yield. To assess the effects of this incomplete infill yielding on the preceding findings, a separate analysis was conducted in which all the strips in the SAP2000 model were removed and replaced by forces of orientation and magnitude equivalent to what would have been developed by the strips had they all been yielded; these results correspond

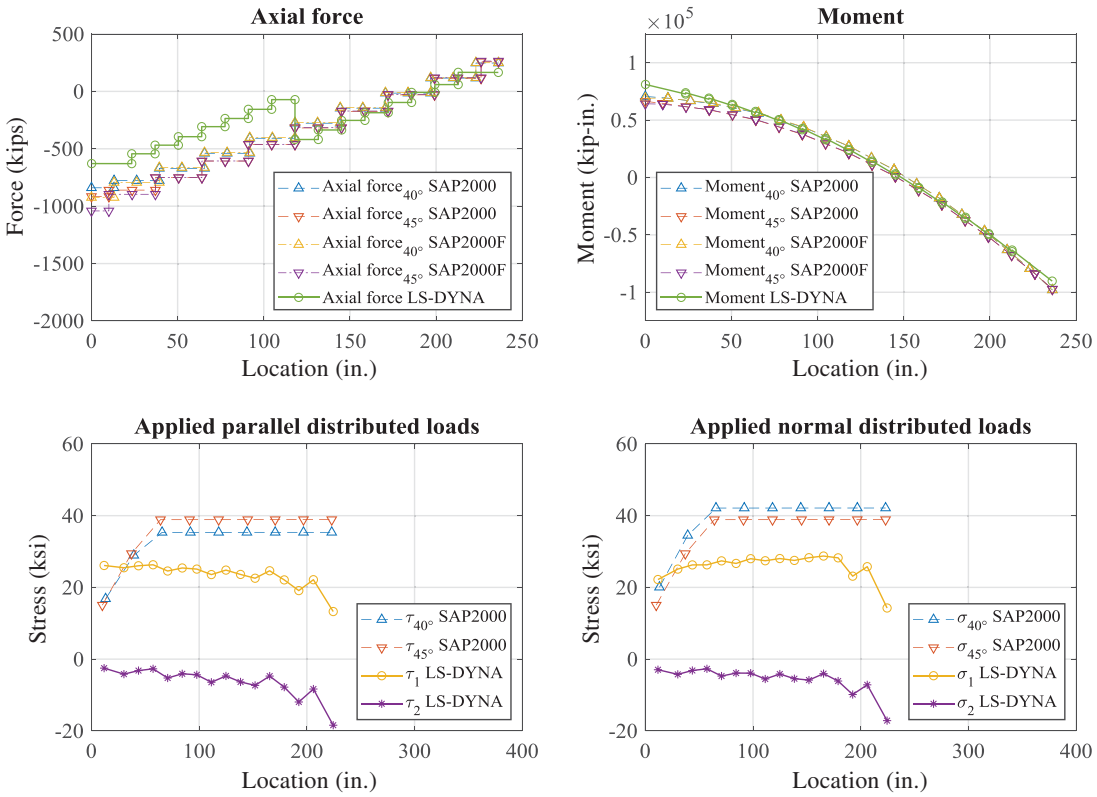

(a)

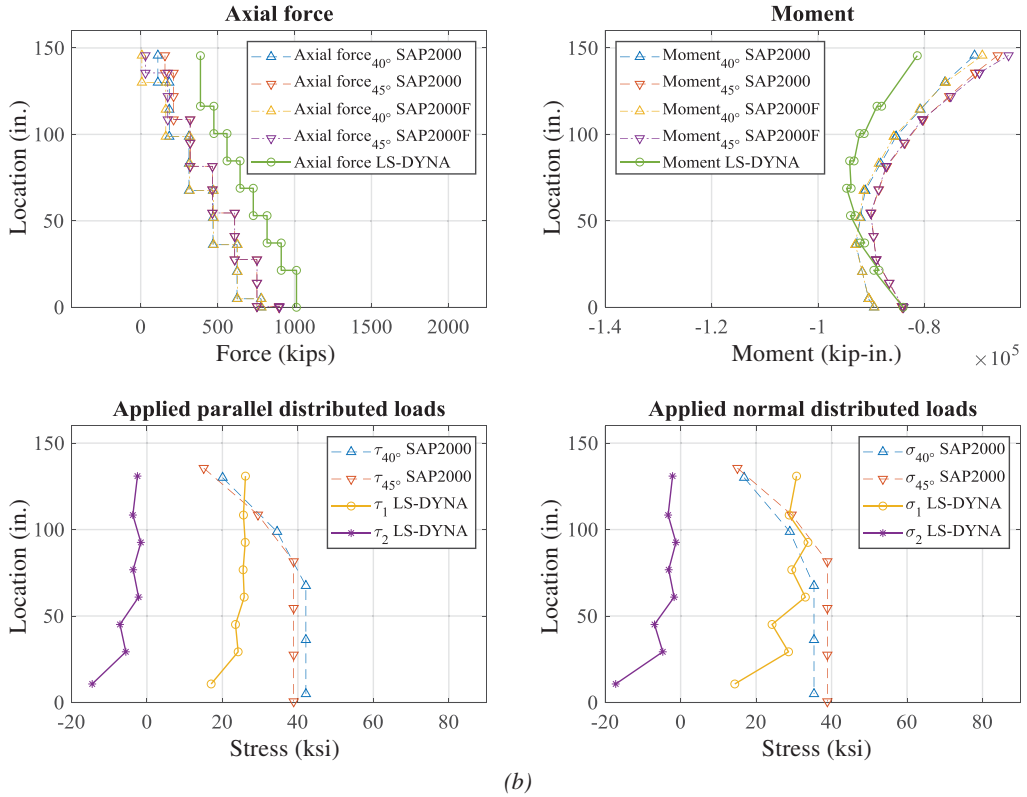

(b)

Fig. 6 (a-b). Comparison of forces obtained from the fourth-story boundary elements in SAP2000 and LS-DYNA: (a) the fourth-story HBE; (b) the fourth-story left VBE.

to the case labeled SAP2000F in Figure 6. Comparing the resulting curves to those obtained from the original strip models, denoted by SAP2000, it is observed that the force and moment diagrams near the corners for the completely and incompletely yielded strip cases are slightly different but that this difference alone merely makes up, at most, a 5% difference between the strip model and the LS-DYNA model in terms of combined axial-moment demand ratio.

The discrepancy on the displacements between the LS-DYNA and SAP2000 models was investigated next. Given the high stiffness of SPSW, a small discrepancy in displacement histories between the SAP2000 strip model and LS-DYNA model is equivalent to applying significant forces at those locations in the FE model. For instance, the discrepancy in displacements between the strip models (SP-40°-U and SP-45°-U) and the LS-DYNA model subjected to the SP-40°-U pushover displacement and loads resulted in a difference in axial force at the fourth HBE's left end of 25.1%, when compared to the strip model using an angle of 40°, and of 31.4%, when compared to the strip model using 45°, as shown in Figure 6(a). Because the combined moment and axial force ratio of this HBE is dominated by the moment term, this eventually led to a net 8% and 12% difference in the ratios per Equation 2 when compared to the results otherwise obtained for the 40°-strip model and 45°-strip model, respectively.

In order to study the influence of the σ_2 effects included in the LS-DYNA model, and the variation of the inclination angle along the boundary elements, the resulting axial forces of the right VBE in the fourth story from the preceding SAP2000 equivalent strip models were compared with those from the LS-DYNA model subjected to SP-40°-U pushover displacements and loads. This is because the difference in axial force diagram accumulated from top to bottom is only due to the σ_2 effects and to the variation in inclination angle along the VBE. By summing up the applied forces parallel to the right VBE, the results from the FE model were found to be less than those obtained from the 45°-strip model by 3.4% and less than the 40°-strip model by 12%.

Although the difference in axial force and moment obtained from SAP2000 and LS-DYNA models was found to be attributed to all of the preceding factors, the demand-to-strength ratios calculated from SAP2000 (denominators) are still comparable to those from LS-DYNA (numerators).

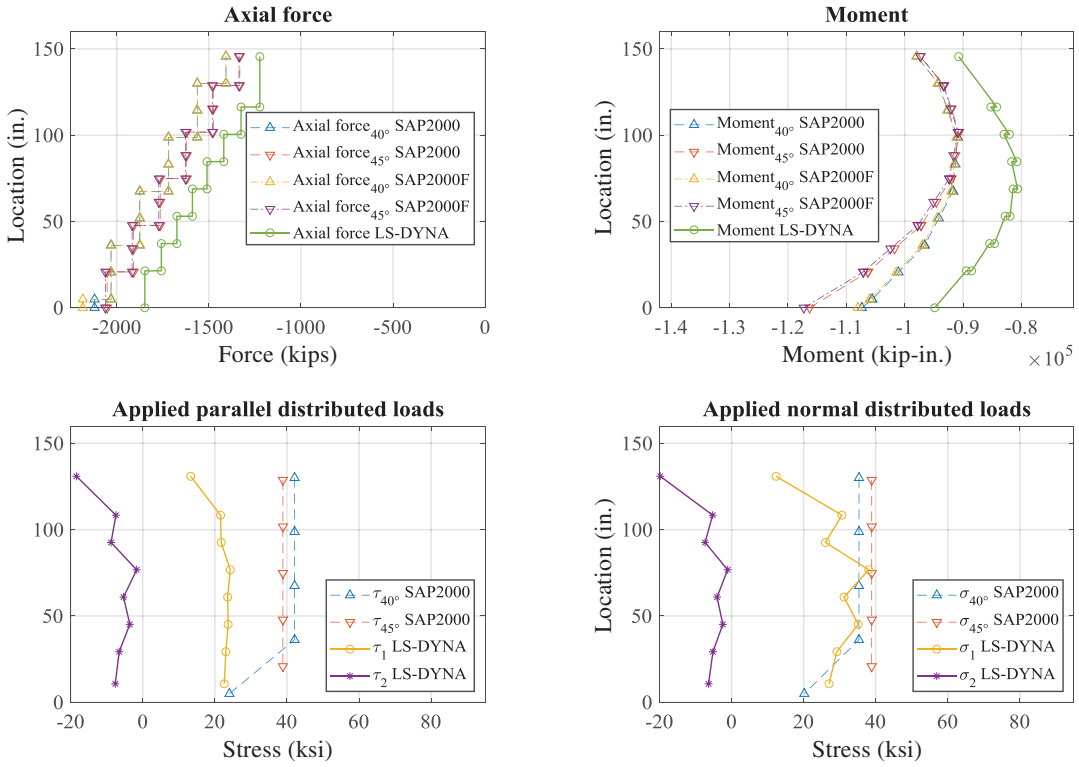

(c)

Fig. 6 (c). Comparison of forces obtained from the fourth-story boundary elements in SAP2000 and LS-DYNA: (c) the fourth-story right VBE. Subscripts "1" and "2" in applied-distributed-loads diagrams represent the maximum principal stress and minimum principal stress obtained from LS-DYNA, respectively.

It is also found that using the inclination angle of 45° is slightly (but not significantly) more conservative than using 40° for boundary element design of the SPSW. Effectively, either 40°or 45° could be used for design.

CONCLUSION

This study expanded on and complemented prior research to determine whether a constant angle of 40° or 45° should be used for the orientation of the tension field action considered in ductile SPSW designed in compliance with the current edition of the AISC *Seismic Provisions* (and of CSA S16). A finite element model was first constructed to replicate a prior study of limited-ductility SPSW, comparing effective stress contours and the average angle of diagonal tension field action at different locations across the web plate. Then, this SPSW was redesigned to have fully restrained beam-to-column connections in compliance with the AISC *Seismic Provisions*, and the finite element model was similarly modified. Pushover analysis results from the finite element model were compared with those obtained from two corresponding strip models analyzed using constant angles of 40° and 45°, respectively. By calculating demands on boundary elements using the AISC moment-axial interaction equation, it was found that using an inclination angle of 45° is slightly (but not significantly) more conservative than using 40° in terms of forces applied to the boundary element of the SPSW. On the basis of these findings, as well as those from previous research investigating the diagonal tension field inclination angle in SPSW, it is found that either 40° or 45° could be effectively used for design of the entire SPSW.

FUTURE RESEARCH

While a limited number of SPSW have been considered here, the previous study by Fu et al. (2017) also showed that 45° was adequate on the basis of demands on VBEs and HBEs on an element-by-element basis due to stresses induced from the web plate only. That prior study considered SPSW having different aspect ratios and number of stories. The more rigorous comparison of true boundary elements forces performed here shows that even when considering the fact that demands on HBEs also affect demands on VBEs (due to shear and axial forces transferred at the ends of HBEs), the recommendation to use 45° remains valid. While the authors are comfortable with this recommendation, future research could investigate the sensitivity of this condition for taller SPSW or other geometries.

REFERENCES

AISC (2005), *Seismic Provisions for Structural Steel Buildings*, ANSI/AISC 341-05, American Institute of Steel Construction, Chicago, IL.

AISC (2010), *Seismic Provisions for Structural Steel Buildings*, ANSI/AISC 341-10, American Institute of Steel Construction, Chicago, IL.

AISC (2016a), *Seismic Provisions for Structural Steel Buildings*, ANSI/AISC 341-16, American Institute of Steel Construction, Chicago, IL.

AISC (2016b), *Specification for Structural Steel Buildings*, ANSI/AISC 360-16, American Institute of Steel Construction, Chicago, IL.

Astaneh-Asl, A. (2001), "Seismic Behavior and Design of Steel Shear Walls," Steel Technical Information and Product Services Report, Structural Steel Educational Council, Moraga, CA.

Behbahanifard, M., Grondin, G. and Elwi, A. (2003), "Experimental and Numerical Investigation of Steel Plate Shear Walls," Structural Engineering Report No. 254, Department of Civil and Environmental Engineering, University of Alberta, Edmonton, AB, Canada.

Berman, J.W. and Bruneau, M. (2004), "Steel Plate Shear Walls Are Not Plate Girders," *Engineering Journal*, AISC, Vol. 41, No. 3, pp. 95–106.

CSA (2001), *Limit States Design of Steel Structures*, CAN/CSA S16-01, Canadian Standards Association, Toronto, ON, Canada.

CSA (2009), *Design of Steel Structures*, CAN/CSA S16-09, Canadian Standards Association, Toronto, ON, Canada.

CSA (2014), *Design of Steel Structures*, CAN/CSA S16-14, Canadian Standards Association, Toronto, ON, Canada.

Choi, I.R. and Park, H.G. (2009), "Steel Plate Shear Walls with Various Infill Plate Designs," *Journal of Structural Engineering*, ASCE, Vol. 135, No. 7, pp. 785–796.

Driver, R.G., Kulak, G.L., Kennedy, D.J.L. and Elwi, A.E. (1997a), "Seismic Behaviour of Steel Plate Shear Walls," Structural Engineering Report No. 215, Department of Civil Engineering, University of Alberta, Edmonton, AB, Canada.

Driver, R.G., Kulak, G.L., Kennedy, D.J.L. and Elwi, A.E. (1997b), "Finite Element Modelling of Steel Plate Shear Walls," *Proceedings of the Structural Stability Research Council Annual Technical Session*, Toronto, ON, Canada, pp. 253–264.

Elgaaly, M., Caccese, V. and Du, C. (1993), "Post-Buckling Behavior of Steel-Plate Shear Walls under Cyclic Loads," *Journal of Structural Engineering*, ASCE, Vol. 119, No. 2, pp. 588–605.

Fu, Y., Wang, F. and Bruneau, M. (2017), "Diagonal Tension Field Inclination Angle in Steel Plate Shear Walls," *Journal of Structural Engineering*, ASCE, Vol. 143, No. 7.

Krawinkler, H. and Seneviratna, G.D.P.K. (1998), "Pros and Cons of a Pushover Analysis of Seismic Performance Evaluation," *Engineering Structures*, Vol. 20, Nos. 4–6, pp. 452–464.

Moghimi, H. and Driver, R.G. (2014a), "Performance-Based Capacity Design of Steel Plate Shear Walls. I: Development Principles," *Journal of Structural Engineering*, ASCE, Vol. 140, No. 12.

Moghimi, H. and Driver, R.G. (2014b), "Performance-Based Capacity Design of Steel Plate Shear Walls. II: Design Provisions," *Journal of Structural Engineering*, ASCE, Vol. 140, No. 12.

Rezai, M. (1999), "Seismic Behavior of Steel Plate Shear Walls by Shake Table Testing," Ph.D. Dissertation, Department of Civil Engineering, University of British Columbia, Vancouver, BC, Canada.

Roberts, T.M. and Sabouri-Ghomi, S. (1992), "Hysteretic Characteristics of Unstiffened Perforated Steel Plate Shear Walls," *Thin-Walled Structures*, Vol. 14, No. 2, pp. 139–151.

Shishkin, J.J., Driver, R.G. and Grondin, G.Y (2005), "Analysis of Steel Plate Shear Walls Using the Modified Strip Model," Structural Engineering Report No. 261, Department of Civil and Environmental Engineering, University of Alberta, Edmonton, AB, Canada.

Timler P.A. and Kulak, G.L. (1983), "Experimental Study of Steel Plate Shear Walls," Structural Engineering Report No. 114, Department of Civil Engineering, University of Alberta, Edmonton, AB, Canada.

Thorburn, L.J., Kulak, G.L. and Montgomery, C.J. (1983), "Analysis of Steel Plate Shear Walls," Structural Engineering Report No. 107, Department of Civil Engineering, University of Alberta, Edmonton, AB, Canada.

Webster, D.J. (2013), "The Inelastic Seismic Response of Steel Plate Shear Wall Web Plates and Their Interaction with the Vertical Boundary Members," Ph.D. Dissertation, University of Washington, Seattle, WA.

Webster, D.J., Berman, J.W. and Lowes, L.N. (2014), "Experimental Investigation of SPSW Web Plate Stress Field Development and Vertical Boundary Element Demand," *Journal of Structural Engineering*, ASCE, Vol. 140, No. 6.